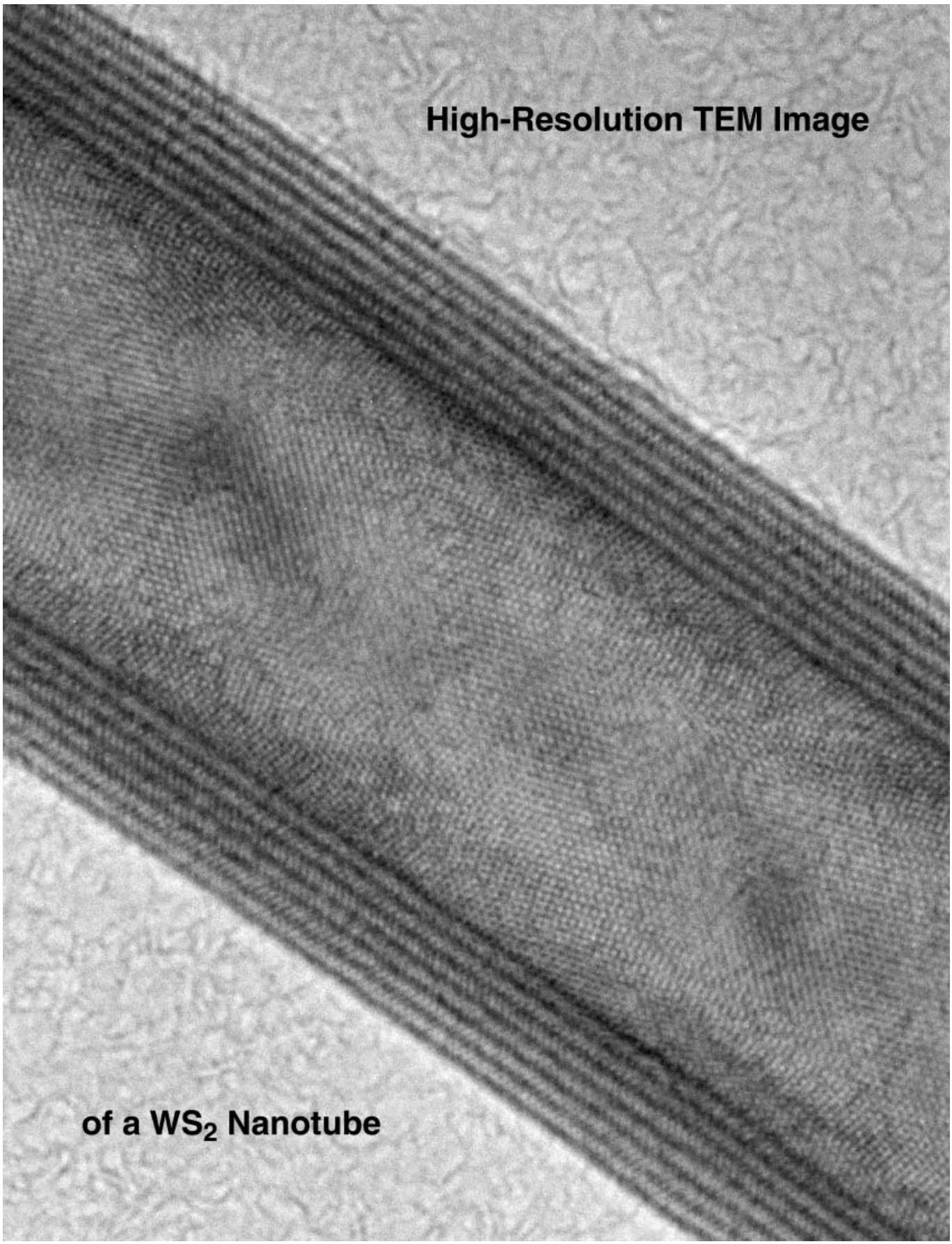

0947-6539/02/0823-5296 $ 20.00+.50/0 *Chem. Eur. J.* **2002**, *8*, No. 23

Inorganic Nanotubes and Fullerene-Like Materials

Reshef Tenne*[a]

Abstract: Following the discovery of fullerenes and carbon nanotubes, it was shown that nanoparticles of inorganic layered compounds, like MoS_2, are unstable in the planar form and they form closed cage structures with polyhedral or nanotubular shapes. Various issues on the structure, synthesis, and properties of such inorganic fullerene-like structures are reviewed, together with some possible applications.

Keywords: inorganic fullerenes · molybdenum · nanostructures · nanotubes · tungsten

Carbon fullerenes and nanotubes

Although graphite is known to be the most stable polytype of carbon, indications for a previously unknown form of carbon came when the high-resolution transmission electron microscopes (TEM) became available during the sixties. Close inspection of carbon soot formed by firing organic materials at elevated temperatures revealed onion-shaped or polyhedral structures, that is, concentric closed graphitic sheets with an empty core. It was perceived in those days that the graphite onions were made "piecewise" of small graphitic platelets held together by an unknown "glue" that stitches the edges and corners of these nanoplatelets together.

The discovery of C_{60} (buckminsterfullerene) by Kroto, Smalley, and Curl in 1985 resolved the mystery of the unknown "glue".[1] In accordance with the Euler rule, the C_{60} molecule was found to be composed of 20 hexagons and 12 symmetrically disposed pentagons. Each pentagon forces the otherwise flat graphitic sheets to distort from the planar structure, and 12 pentagons provide sufficient bending to close the entire plane into a hollow structure. Following this discovery, many other fullerenes and related forms of carbon, in particular nanotubes,[2] were proposed and found. Carbon nanotubes are made of rolled graphene sheets capped with half a fullerene molecule of the same diameter at each of the two ends. Therefore these structures can be viewed as an elongated form of a fullerene. Both fullerenes and nanotubes are seamless structures that contain carbon atoms that only form bonds to three other atoms. The absence of dangling bonds renders these structures energetically very stable. Nonetheless, the deviation from planarity induces a non-negligible amount of stress into the fullerenes; this explains many of their chemical and physical properties.

[a] Prof. R. Tenne
Department of Materials and Interfaces
Weizmann Institute, Rehovot 76100 (Israel)
Fax: (+972) 8-93-44138
E-mail: reshef.tenne@weizmann.ac.il

Are there inorganic analogues?

The driving force for the formation of carbon fullerenes and nanotubes stems from the abundant reactive atoms on the periphery of the quasi two-dimensional planar nanostructure. These edge atoms only form bonds to two other atoms rather than three as in the bulk (see Figure 1). Thus, the planar topology of graphene nanoparticles is unstable with respect to the hollow and seamless fullerenes. By using similar reasoning, it has been proposed [3, 4] that the formation of fullerenes is not unique to carbon and is a genuine property of two-dimensional (layered) compounds. Inorganic layered compounds are abundant, in particular among the transition-metal chalcogenides (sulfides, selenides, and tellurides), halides (chlorides, bromides, and iodides), oxides, and numerous ternary (quaternary) compounds. However in contrast to graphite, each molecular sheet consists of multiple layers of different atoms chemically bonded together.

If one considers MoS_2 as an example (see Figure 1), each molecular sheet is made of a layer of molybdenum atoms sandwiched between two outer sulfur layers. The Mo atoms form six bonds to sulfur atoms to form a trigonal biprism. In analogy to graphite, weak van der Waals forces are responsible for the stacking of the S-Mo-S layers together. Like graphite, such compounds are highly anisotropic with respect to many of their physical and chemical properties. The (van der Waals) surfaces of the crystal, which are perpendicular to the *c* axis, consist of sulfur atoms that form bonds to three other atoms; these sulfur atoms are not chemically reactive. In contrast to the fully bonded bulk sulfur and molybdenum atoms, these atoms are not fully bonded on the plane's edges, that is, the prismatic faces (parallel to the *c* axis) and are, therefore, chemically very reactive. Indeed, each

  0947-6539/02/0823-5297 $ 20.00+.50/0

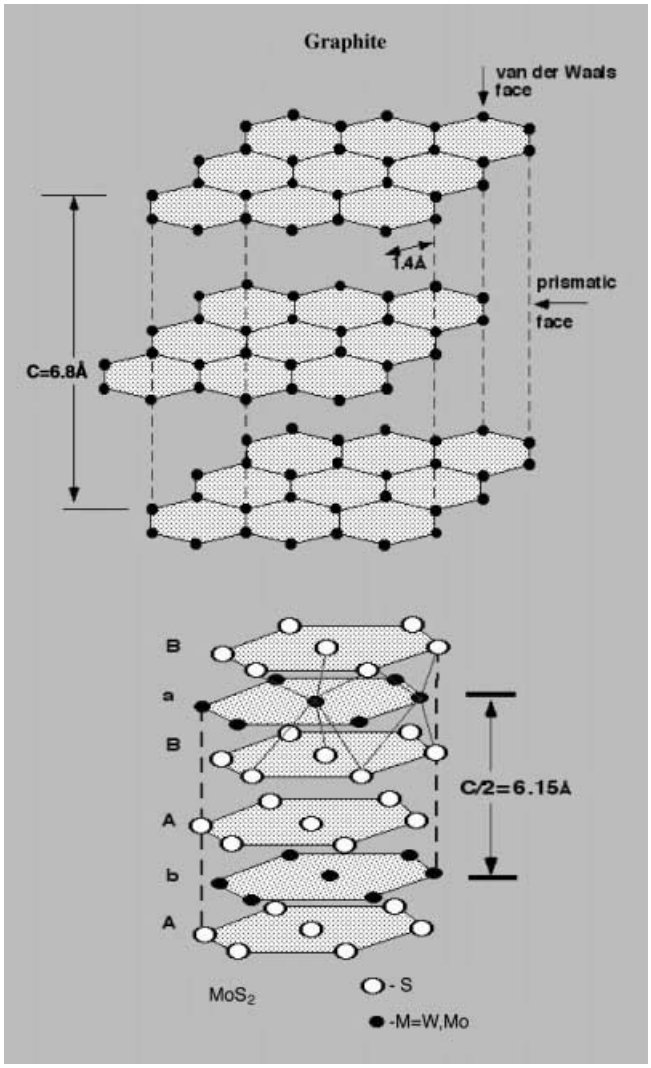

Figure 1. Schematic drawings of graphite and MoS_2 nanoclusters. Note that in both cases, the surface energy, which destabilizes the planar topology of the nanocluster, is concentrated in the prismatic edges parallel to the *c* axis.

molybdenum atom in the prismatic (100) edge is bound to only two sulfur atoms of the upper plane and two sulfur atoms of the lower plane (see Figure 1). Therefore each Mo atom on the (100) face has two dangling bonds and is consequently chemically reactive. On the opposite face (−100) of the MoS_2 platelet, the sulfur atoms form only two bond to two other atoms and they possess one dangling bond per sulfur atom. Therefore, the Mo atoms of the (100) face would tend to recombine with the S atoms at the opposite side of the platelet. Since the ratio between peripheral (partially bonded) and bulk (fully bonded) molybdenum (sulfur) atoms increases with shrinking size of the platelet (sheet), nanoparticles of MoS_2 are not expected to be stable in the planar form and they fold to form closed-cage nanostructures. This hypothesis has been invariably confirmed by both experiment and theory. Extensive experimental data available now tend to substantiate this initially intuitive hypothesis and show that this new curved and hollow phase of layered compounds, designated as inorganic fullerene-like (IF) material, is the thermodynamically stable form, given the constraint that the particles can not grow beyond about 0.2 μm. Energy must be provided, initially, to overcome the activation barrier ensuing from the elastic energy of bending of the otherwise planar sheet. In most cases thermal energy has been used for this purpose, but other energy sources, like irradiation, microwave, sonochemical, and electrical energy were also found to be adequate for the activation of the nanoparticle folding process.

Figure 2 shows transmission electron microscopy (TEM) images of typical MoS_2 (a) and WS_2 (b) hollow nanoparticles (onions) that consist of more than ten molecular MoS_2 layers

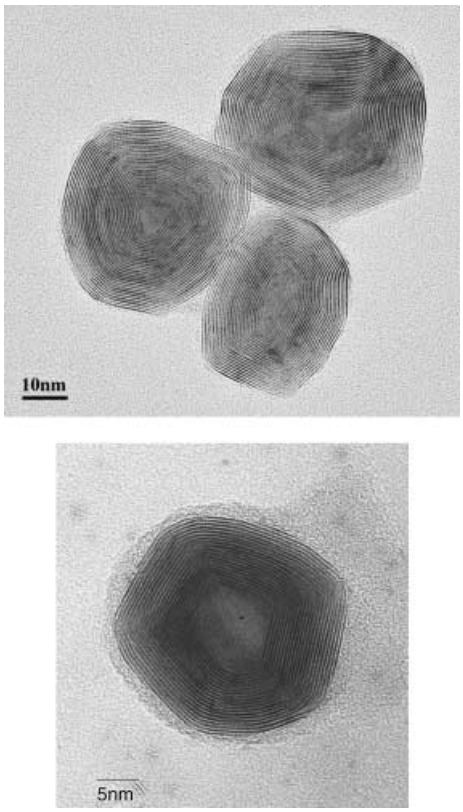

Figure 2. TEM image of typical MoS_2 (top) and WS_2 (bottom) nanoparticles with fullerene-like structure. Each dark line represents an atomic layer of the basal plane (001). The distance between two layers is 6.18 Å. The *c* axis is always normal to the surface of the nested fullerene-like structure.

arranged in a concentric seamless form. Such nested (fullerene-like) structures are produced by the tens of grams daily in the Weizmann Institute laboratory. Figure 3 shows typical TEM images of multiwall WS_2 nanotubes. Nanotubes of this kind are currently produced by the gram, although not yet in a pure phase.

Synthesis

Inorganic fullerene-like nanoparticles: In order to obtain pure IF phases, it is imperative to prevent the nanocrystallites from growing beyond a certain size during the process (arrested growth). Numerous methods have been conceived for this purpose. Multigram quantities of IF-WS_2 and smaller amounts of IF-MoS_2 can be grown from the respective oxide phases.[5]

0947-6539/02/0823-5298 $ 20.00+.50/0 *Chem. Eur. J.* **2002**, *8*, No. 23

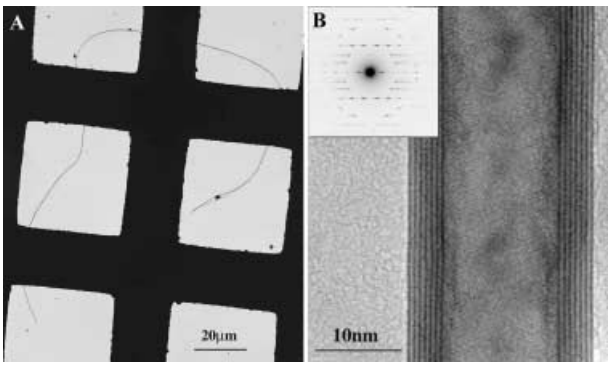

Figure 3. TEM micrographs of a) a bundle of three very long WS_2 nanotubes, and b) a high-resolution image of a WS_2 nanotube, and its electron diffraction (inset) showing the helicity of the nanotube (from ref. [13], reproduced with permission of the ACS).

A schematic diagram of the growth process is edpicted in Figure 4. First, nanoparticles of the oxide phase are obtained. MoO_3 nanoparticles are obtained in situ by evaporating MoO_3 powder at 800 °C and subsequently reducing the vapor in a hydrogen gas at about 820 °C. In the next step, which lasts about a second, the heated oxide nanoparticles react with H_2S gas at 840 °C and are sulfidized at the surface. The sulfide encapsulated oxide nanoparticles have passivated surfaces and cannot grow further. Subsequently, in a rather slow diffusion-controlled process, the entire oxide core of the nanoparticles is converted into a metal disulfide in a highly uniform and regular fashion at 840 – 950 °C. The key element in the success of this strategy is that during this high-temperature process the incipient oxide nanoparticles are allowed to interact with the carrier (N_2) and H_2 gases, but their interaction with each other is mostly excluded before they are passivated by the reaction with H_2S; this leads to the formation of a protective sulfide top layer. Once this protective layer has been formed, the completion of the oxide to sulfide conversion can be done in the bulk, that is, without isolation of the nanoparticles.

WO_3 is much less volatile than MoO_3, and hence the precursors for IF-WS_2, that is, the tungsten oxide nanoparticles, cannot be formed by sublimation. Therefore, a pre-prepared WO_3 powder with particle sizes of 0.02 – 0.2 μm was used here. These small tungsten oxide nanoparticles can be prepared by a number of ways, for example, by heating a tungsten filament to 1600 °C inside an evacuated bell jar in the presence of water vapor, or by calcination of tungstic acid. Once the details of the reaction mechanism were unraveled, a fluidized-bed reactor for the synthesis of more than 40 g per day of a pure phase of fullerene-like WS_2 nanoparticles could be established.[6]

A different strategy has been employed for the synthesis of fullerene-like NbS_2 nanoparticles. Here an $NbCl_5$ precursor was preheated to 200 °C first and its vapor was swept into the main reactor by an inert carrier gas (N_2).[7] A gas mixture consisting of H_2, N_2, and H_2S was provided separately to the reactor and reacted with the $NbCl_5$ vapor at around 450 °C. The synthesized IF-$Nb_{1+x}S_2$ nanoparticles were covered by an amorphous layer, which could be crystallized by further annealing at 550 °C for two hours. A typical product of this reaction is shown in Figure 5. One typical aspect of the IF-NbS_2 nanoparticle morphology is its highly faceted shape, which is discussed below. The scalability of this reaction is yet to be demonstrated.

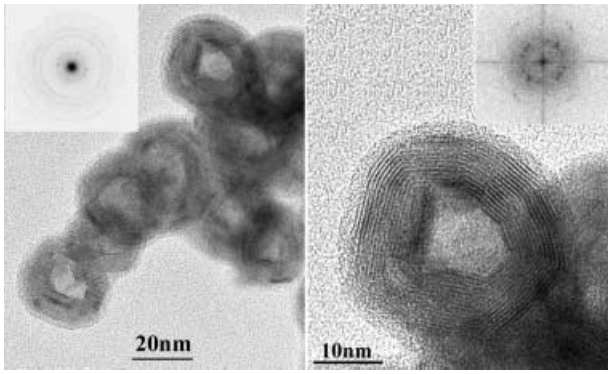

Figure 5. TEM of NbS_2 nanoparticles with fullerene-like structure after annealing. Inset on the left side shows the electron diffraction pattern of a group of nanoparticles, while inset on the right hand side shows Fourier transform done on a single NbS_2 nanoparticle. Note the strong faceting of the nanoparticles (from ref. [7], reproduced with permission of the RSC).

In a different series of experiments, fullerene-like $CdCl_2$[8] and $NiCl_2$[9] nanoparticles were produced by a few different processes. Both compounds crystallize in the layered $CdCl_2$ ($R\bar{3}m$) structure, but due to the large polarization of the metal – chlorine bond, they are highly hygroscopic. Interestingly, while bulk $CdCl_2$ is highly hygroscopic, the IF-$CdCl_2$ nanoparticles obtained through electron beam irradiation of $CdCl_2 \cdot H_2O$ powder (see Figure 6) become water resistant for very long periods. This observation underpins the importance of the kinetic stabilization against hostile conditions; this is provided by the seamless structure of the nanoparticles. Two kinds of structures are typically observed for these

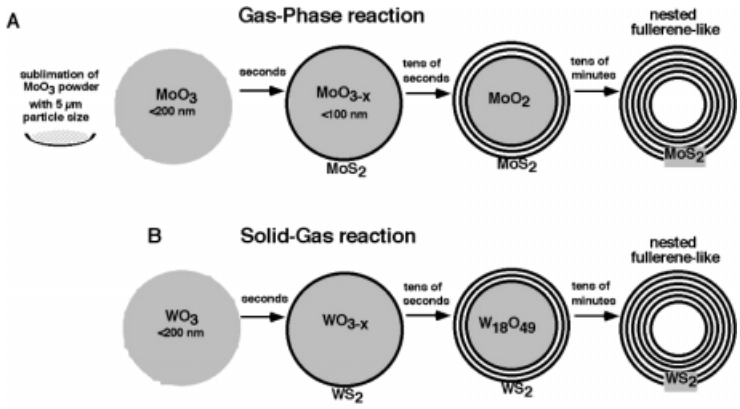

Figure 4. A schematic drawing of the growth process of fullerene-like MoS_2 (WS_2) from the respective oxides (adapted from ref. [5]).

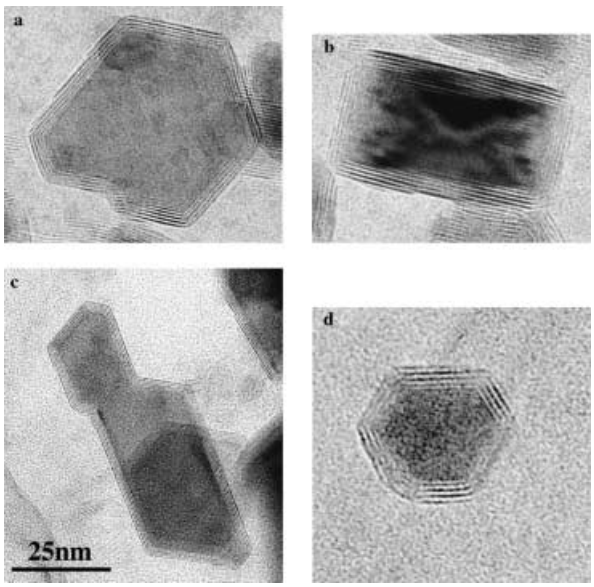

Figure 6. TEM of multilayer $CdCl_2$ nanoparticles with a closed cage structure. Note the two most architypical structures, that is, hexagon and rectangle (from ref. [8], reproduced with permission of the editors of *Isr. J. Chem.*).

closed polyhedra, one with hexagonal shape (Figure 6a, c, and d) and the other with rectangular structure (Figure 6b). Figure 7 depicts a possible structure that affords the two observed projections in one polyhedron. However, this schematic structure does not reveal the exact position of each atom at the corners of the polyhedron (see below).

By using a sonochemical bath, nanoparticles of the layered compound Tl_2O with anti-$CdCl_2$ structure were synthesized in substantial amounts as shown in Figure 8. They were later isolated by selective heating of the reaction product to 300 °C.[10] In contrast to the unstable bulk material, the seamless structure of the nanoparticles provides a kinetic stabilization. Thus the closed nanoparticles do not expose the prismatic edges, and, thesrefore, are protected against exfoliation by water intercalation into the van der Waals gaps, or thermal decomposition during the purification step.

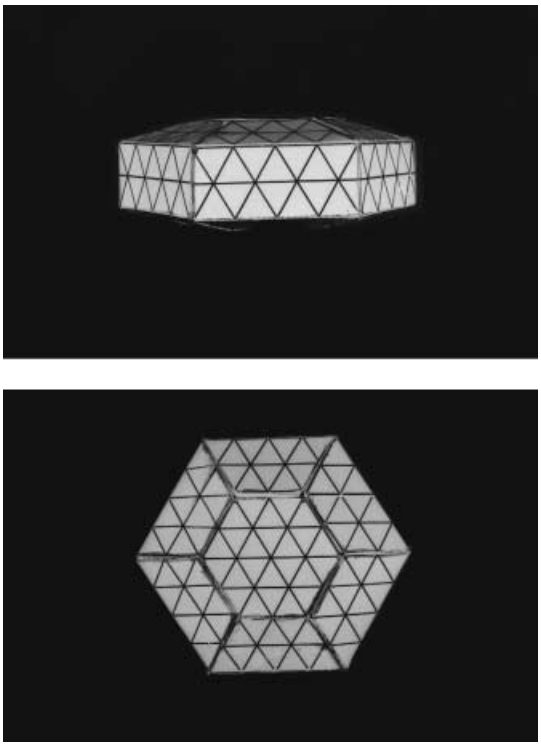

Figure 7. Schematic representation of the hypothized $CdCl_2$ polyhedron (from ref. [8], reproduced with permission of the editors of Isr. J. Chem.).

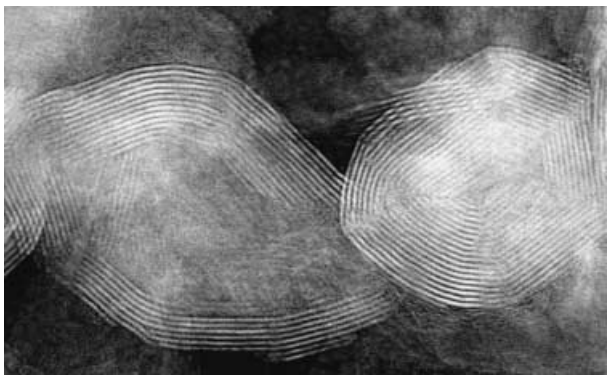

Figure 8. TEM image of Tl_2O onions obtained by a sonochemical reaction of $TlCl_3$ in aqueous solution. The distance between the lattice fringes is 6.4 Å. Courtesy of A. Gedanken.

Nanotubes: In early reports only minor amounts of WS_2,[3], MoS_2,[11] and BN[12] nanotubes could be produced. However recently, various strategies have been successfully employed for the synthesis of large amounts of various nanotubes. Thus, by using a fluidized-bed reactor, synthesis of gram quantities of very long WS_2 nanotube phases was accomplished.[13] Figure 3a shows a bundle of three very long nanotubes of this kind. The high-resolution image of one such long and quite perfect nanotube is shown in Figure 3b together with the electron diffraction of the nanotube in the inset. With regard to the growth mechanism of such nanotubes, in accordance with existing literature, it is believed that in the first instant of the reaction the quasi-spherical tungsten oxide nanoparticles are transformed into tungsten oxide nanowhiskers. Subsequently, the oxide nanowhiskers are converted into WS_2 nanotubes, by a process similar to the one described in the previous section for the synthesis of fullerene-like WS_2 nanoparticles. This hypothesis is supported by the two-step growth process, in which the oxide nanowhisker phase is obtained in the first step, and is subsequently converted to WS_2 nanotubes phase in an H_2S atmosphere.[14] Uniform WS_2 nanotubes were also obtained by the chemical vapor transport (CVT) technique,[15] in which the WS_2 powder is transported from the hot to the colder zones of a quartz ampoule by means of a transporting agent, for example, iodine. Extremely uniform and very long single-wall MoS_2 nanotubes with diameter of less than 1 nm have also been synthesized.[16] These nanotubes crystallize in the armchair (3,3) configuration. Their perfectness can be also gauged by the fact that they self-assemble into a hierarchy of higher order structures, from the single nanotube level to macroscopic crystallites.[16] Interestingly, these nanotubes were obtained through a CVT process with C_{60} as a catalyst. This process is quite slow and will probably not be suitable for large scale synthesis of these kinds of nanotubes. It remains to be shown if this process can

0947-6539/02/0823-5300 $ 20.00+.50/0 *Chem. Eur. J.* **2002**, *8*, No. 23

be modified to obtain nanotubes of different diameter and chirality. Nanotubes from various metal disulfide compounds, including NbS_2 and TaS_2, were synthesized by high-temperature annealing of the respective ammonium thiometallates.[17] Double-wall boron nitride nanotubes of high uniformity were produced by the arc-discharge method.[18] V_2O_5 nanotubes were synthesized by using organic amines as templating molecules in a sol-gel process followed by hydrothermal treatment.[19] The use of "chimie douce" proccesses for the preparation of new kinds of nanotubes from a number of oxide compounds has been accomplished. Thus, scroll-like nanotubules have been obtained from potassium hexaniobate ($K_4Nb_6O_{17}$) by acid exchange and careful exfoliation in basic solution.[20, 21] The exfoliation process results in monomolecular layers, which are unstable against folding, even at room temperature, and consequently form the more stable scroll-like structures. Moreover, although the binary oxides of these transition metals do not possess the lamellar structure and, consequently, cannot form crystalline nanotubular structures, the reduced oxides of these phases can. A typical example belonging to this category is the compound $H_2Ti_3O_7$, which belongs to the class of reduced lamellar $H_2Ti_nO_{2n+1}$ phases, which was shown to exhibit lamellar structures and form perfectly crystalline nanotubes.[22] This nanotubular phase was prepared by the usual sol–gel process and subsequent treatment with a concentrated NaOH solution at 130 °C. Numerous other strategies were employed for the synthesis of these and other inorganic nanotubes in recent years. These works demonstrate the richness of the chemical apparatus in the context of inorganic nanotubes and fullerene-like nanostructures.

Structures of IF Nanoparticles

C_{60}, which is made of hexagons and pentagons only, exhibits icosahedral symmetry. The trigonal prismatic structure of MoS_2 (and many other layered compounds) offers a new kind of folding mechanism. Neither graphite nor MoS_2 have pentagonal elements within their native structure. Notwithstanding, triangles and rectangles form a genuine element of lower symmetry within the trigonal network of MoS_2. It was therefore proposed,[4] and later on experimentally confirmed,[23] that MoS_2 octahedra (bucky-octahedra) made of six symmetrically disposed rectangular corners can be obtained. Similarly, in one case a MoS_2 "bucky-tetrahedron" made of symmetrically disposed four triangles was observed. These structures are likely to be the most stable form of IF-MoS_2 nanoparticles, that is, the analogue of C_{60} in MoS_2. Figure 9 shows the TEM and the simulated image of one such octahedron tilted at various angles.

Boron nitride nanotubes and fullerene-like nanoparticles were among the early non-carbon systems to be studied. Boron is situated to the left of carbon in the periodic table, while nitrogen is to its right. In analogy to carbon, boron nitride (BN) exists in two main phases: hexagonal (graphite-like) and cubic (diamond-like). Moreover, the stable form of BN at room temperature is the graphitic (hexagonal) polytype. Therefore, nanoparticles of this phase are expected to be

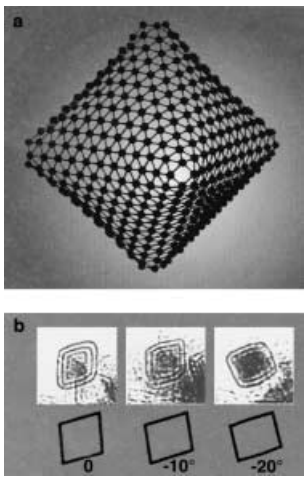

Figure 9. a) Structural model of the octahedron containing 592 Mo atoms. b) TEM images and simulated projections for a MoS_2 octahedron tilted at 0, 10 and 20° (adapted from ref. [20]).

unstable in the planar form, affording the fullerenic structure. This hypothesis has been verified experimentally in various laboratories. Energy considerations show that B–B or N–N are not favorable nearest neighbors, and consequently the folding of the hexagonal BN network is done by introducing six $(BN)_2$ rectangles, rather than 12 pentagons, into the hexagonal network. The smallest stable fullerene-like structure was calculated to be $B_{12}N_{12}$,[24] which is schematically represented in Figure 10. Both BN octahedra (six rectangles) [25] and nanotubes, with flat tops that consist of three rectangles,[26] have indeed been synthesized by various methods.

An elastic continuum model, which takes into account the energy of bending, the dislocation energy, and the surface energy, was used in order to describe the mechanical properties of multilayer cage structures to a first approximation.[27] A

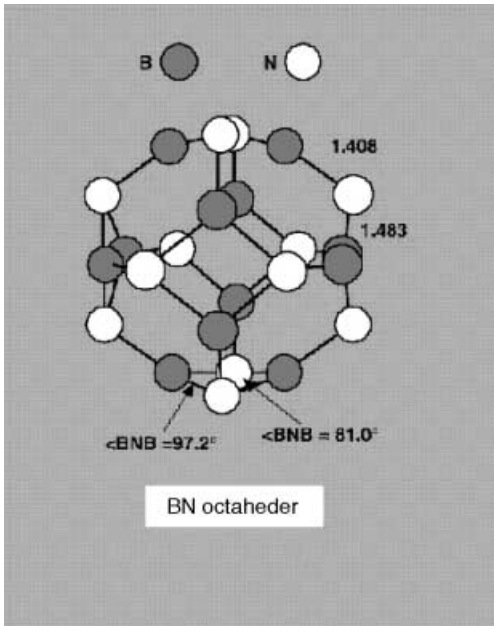

Figure 10. Schematic diagram of a $B_{12}N_{12}$ octahedron (adapted from ref. [21]).

  0947-6539/02/0823-5301 $ 20.00+.50/0

first-order phase transition from an evenly curved (quasi-spherical) structure into a polyhedral cage was predicted for WS_2 (MoS_2) nested fullerenes with shell thickness larger than about 1/10 of the nanotube radius. Indeed, such a transition was observed during the synthesis of IF-WS_2 particles.[5] Initially the oxide nanoparticles enveloped with a few WS_2 molecular layers were found to be quasi-spherical. They transformed into a faceted structure when the thickness of the sulfide shell in the nanoparticles exceeded a few nanometers. Also in accordance with this theory, NbS_2, which has a bending modulus larger than that of WS_2, crystallizes in a highly faceted fashion, as shown in Figure 5.[7] Moreover, the highly polar bonds of the layered metal chlorides lead to bending moduli almost an order of magnitude larger than that of MoS_2 (WS_2). Not surprisingly, these nanoparticles afford highly faceted polyhedra, as demonstrated in Figure 6.[8] In the case of IF-$NiCl_2$,[9] one-layer thick polyhedra were found to fold either in quasi-spherical or in faceted (polyhedra) forms, while three-layers thick polyhedra are invariably highly faceted. The formation of nanotubes requires folding in one direction only, and, hence, involve appreciably lower elastic strain. It is therefore not surprising that inorganic nanotubes are generally cylindrical and only rarely were they found to be faceted. Evidently, this theory cannot provide the accurate arrangement of the atoms in the corners or the polyhedra.

The topology of single-layer polyhedra has been investigated virtually for hundreds of years. In contrast, the study of polyhedra that consist of a number of interconnected layers with fixed lattice points in each layer, which is a common place in IF structures, has been barely studied. This challenging issue is clearly demonstrated in the case of IF-$CdCl_2$, in which only partial information regarding the structure of the polyhedron is available (see Figures 6 and 7). Furthermore, realistic models of IF structures, like MoS_2 octahedra that consist of some 1800 atoms, require highly developed ab initio calculations; at present this makes the task quite intractable. Some progress in this direction is discussed in reference [28]. Therefore, the synthesis and elucidation of the structure of IF nanoparticles remains a most challenging task for the years to come.

Properties

Some of the properties of inorganic nanotubes and fullerene-like materials have been elucidated by both theory and experiment. Early theoretical work was concerned with BN, BC_2N, and BC_3 nanotubes (see for example ref. [29]). More recent work has concentrated on nanotubes of other compounds, such as phosphorous,[30] GaSe,[31] and MoS_2.[28] The picture emerging from these studies is that nanotubes of compounds which are semiconducting in the bulk form maintain this character after folding. Nonetheless, the strain involved in the folding of the molecular sheets, which is often an order of magnitude larger than for carbon nanotubes, leads to the shrinkage of the semiconductor bandgap with decreasing diameter of the nanotube. Therefore, the bandgap of semiconducting nanotubes can be tuned all the way from the UV spectrum (ca. 3 eV) down to the infrared (ca. 0.2 eV) by varying the diameter of the nanotubes. This behavior is to be contrasted with the generic expansion of the bandgap with a decrease in the diameter of semiconductor nanoparticles, due to the quantum size effect.

This behavior was confirmed by measurements of the absorption spectrum of IF-MoS_2 and IF-WS_2.[32] More recently, scanning tunneling microscopy was used for high-resolution imaging of WS_2 nanotubes. In addition, I-V curves for each of the imaged nanotube were recorded, from which the energy gap as a function of the nanotube diameter could be deduced.[33] Figure 11 presents a comparison between

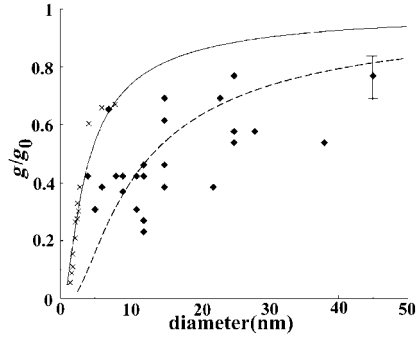

Figure 11. Comparison between theory and experimental data of the normalized bandgap (g/g_0) of WS_2 nanotubes with varying diameters. g_0 is the energy gap of the bulk materials (1.2 eV). Note the scattering in the experimental data, which nevertheless provides a faithful description of the dependence of the bandgap on the nanotube diameter. Reproduced with permission of the PCCP owner societies

theory and experiment. While large scattering in the experimental data is observed, a qualitative agreement between theory and experiment is unfolded. Furthermore, in correspondence with the electronic structure of bulk (2H-MoS_2), the theory also indicates that armchair nanotubes possess an indirect bandgap for the lowest electronic transition.[28] However, from theory, zig-zag nanotubes are expected to exhibit a direct transition. This surprising observation suggests that such nanotubes could show strong optical absorption and luminescence, or even stimulated emission (laser action). Theory also shows that, independent of their diameter and chirality, NbS_2 nanotubes are metallic, which suggest that they will be very good field emitters of electrons.[34]

Applications

2H-MoS_2 (2H-WS_2) is an ubiquitous solid lubricant, serving as an additive to heavy-duty fluids, coatings, or as lubricating powders in ultra high-vacuum instrumentation. Unfortunately, 2H-MoS_2 platelets tend to adhere to the metal surfaces through their reactive edges (i.e., the prismatic faces), in which configuration they "glue" the two metal surfaces together rather than serving as solid lubricant. Abrasion of the solid lubricant during the mechanical action naturally leads to a reduced particle size. The smaller the MoS_2 platelets are, the greater is their tendency to stick to the metal surfaces through their reactive edges. Therefore the tribological benefits of MoS_2 crystallites vanish quite rapidly. The

0947-6539/02/0823-5302 $ 20.00+.50/0 *Chem. Eur. J.* **2002**, *8*, No. 23

spherical shape of the fullerene-like nanoparticles and their inert sulfur-terminated surfaces offer advantageous tribological properties for solid lubricants made of such nanoparticles. The spherical IF-MS_2 particles are expected to behave like nano-sized ball bearings, and upon extensive mechanical stress they would slowly exfoliate or mechanically deform into a rugby-shaped ball, but would not lose their tribological action until complete disappearance. The usefulness of IF powders as solid lubricants has been confirmed through a long series of experiments in the laboratory of Rapoport.[35] Further experiments, in which IF-WS_2, and later on IF-MoS_2, powders were tested under different experimental modalities and various experimental conditions indicate that such nanoparticles are superior solid lubricants providing self-lubricity to various coatings,[36] bearings,[37] etc. Figure 12 shows the results of a tribological test in which part of a

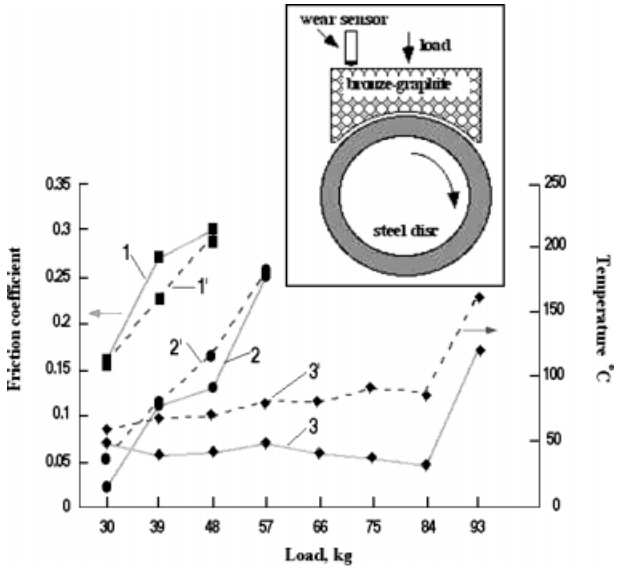

Figure 12. Friction coefficient (1,2,3) and temperature (1′,2′,3′) versus load (in kg) of porous bronze-graphite block against hardened steel disk (HRC 52). In these experiments, after a run-in period of 10–30 hours, the samples were tested under a load of 30 kg and sliding velocity of 1 $m s^{-1}$ for 11 h. Subsequently, the loads were increased from 30 kg with an increment of 9 kg and remained 1 h under each load. (1,1′) bronze-graphite sample without added solid- lubricant; (2,2′) bronze graphite sample with 2H-WS_2 (6%); (3,3′) the same sample with (5%) hollow (IF) WS_2 nanoparticles.

bronze-graphite sample prepared by powder metallurgy and impregnated with 5% IF-WS_2 outperforms the non-impregnated part. Thus, addition of only 5% IF-WS_2 nanoparticles led to a remarkable improvement in the load-bearing capacity of the tested part. This experiment, and numerous others carried out over the past few years, suggests a possible application for these nanoparticles both as additives in lubrication fluids or greases and in composites with metals, plastics, rubber, ceramics, and numerous other surfaces.

Another important field in which inorganic nanotubes can be useful is as tips in scanning probe microscopy and for nanotechnology. Here inspection of microelectronic circuitry elements has been demonstrated and potential applications in nanolithography are being contemplated. Although other kinds of tips have been in use in recent years for high-resolution imaging by scanning probe microscopy, the inorganic nanotube tips, by virtue of their stiffness and inertness, are likely to serve well in the high-resolution imaging of rough surfaces that have features with a large aspect ratio. Furthermore, the strong absorption of light in the visible part of the spectrum makes these nanotubes suitable for nanolithography and near-field optical imaging. Magnetic nanotubes, for example, from $NiCl_2$ nanotubes, could find applications in data storage and retrieval. NbS_2 nanotubes have been predicted to have large density of states in the Fermi level; this suggests that they will be good field emission sources of electrons.

Recently, substantial interest has been paid to metal and hydrogen intercalation in inorganic nanotubes of various kinds. Thus, Li intercalation and deintercalation in V_2O_5 and $Mn_xV_2O_{5+x}$ nanotubes was studied. Potassium and sodium intercalation in MoS_2 (WS_2) fullerene-like nanoparticles was also investigated. Reversible hydrogen loading and discharge in MoS_2 nanotubes was demonstrated.[38] The relatively facile loading/discharge of the intercalated metals and hydrogen can be attributed to the high surface area and the open tips of the nanotubes. The high level of organization in the nanoparticles' structure is potentially important in order to accomplish numerous charge/discharge cycles of the rechargeable electrode, without losing their loading capacity. Catalytic conversion of $CO + H_2$ into methane and water by using MoS_2 nanotubes as catalyst was recently demonstrated.[39] The mechanism of the catalytic action of the nanotubes is quite a puzzle, since the fully bonded sulfur atoms in the van der Waals surfaces and in the galaries of the MoS_2 layers (van der Waals gap) of the nanotubes are not expected to be chemically very reactive. This surprising result is nevertheless promising enough to incite new research effort into the catalytic properties of inorganic nanotubes.

In conclusion, the advent of nanotubes and fullerene-like particles from inorganic layered compounds has opened new avenues in the solid-state chemistry of inorganic compounds and new opportunities for application of such nanostructures in the emerging field of nanotechnology as well as in numerous other areas. Fundamental questions remain to be solved in order to permit a more judicious approach to the synthesis and study of the properties of these new nanophase materials. The elucidation of the detailed structure of IF nanoparticles is progressing by a combination of theory and experiment.

Acknowledgements

I am grateful to Y. Feldman, A. Zak, A. Margolin, R. Rosentsveig, Y. Rosenfeld Hacohen, R. Popovitz-Biro, and L. Rapoport. Support of the Israeli Ministry of Science (Tashtiot), Israeli Academy of Sciences (First), the Israel Science Foundation, and Minerva Foundation (Munich) are gratefully acknowledged.

[1] H. W. Kroto, J. R. Heath, S. C. O'Brien, R. F. Curl, R. E. Smalley, *Nature* **1985**, *318*, 162.
[2] S. Iijima, *Nature* **1991**, *354*, 56.
[3] R. Tenne, L. Margulis, M. Genut, G. Hodes, *Nature* **1992**, *360*, 444.

[4] L. Margulis, G. Salitra, R. Tenne, M. Talianker, *Nature* **1993**, *365*, 113.
[5] Y. Feldman, G. L. Frey, M. Homyonfer, V. Lyakhovitskaya, L. Margulis, H. Cohen, G. Hodes, J. L. Hutchison, R. Tenne, *J. Am. Chem. Soc.* **1996**, *118*, 5362.
[6] Y. Feldman, A. Zak, R. Popovitz-Biro, R. Tenne, *Solid State Sci.* **2000**, *2*, 663.
[7] C. Schoffenhauer, R. Popovitz-Biro, R. Tenne, *J. Mater. Chem*. **2002**, 1587.
[8] R. Popovitz-Biro, A. Twersky, Y. Rosenfeld Hachoen, R. Tenne, *Isr. J. Chem*. **2001**, *41*, 7.
[9] Y. Rosenfeld Hacohen, E. Grunbaum, R. Tenne, J. Sloan, J. L. Hutchison, *Nature* **1998**, *395*, 336.
[10] S. Avivi, Y. Mastai, A. Gedanken, *J. Am. Chem. Soc*. **2000**, *122*, 4331.
[11] Y. Feldman, E. Wasserman, D. J. Srolovitz, R. Tenne, *Science* **1995**, *267*, 222.
[12] N. G. Chopra, J. Luyken, K. Cherry, V. H. Crespi, M. L. Cohen, S. G. Louie, A. Zettl, *Science* **1995**, *269*, 966.
[13] R. Rosentsveig, A. Margolin, Y. Feldman, R. Popovitz-Biro, R. Tenne, *Chem. Mater*. **2002**, *14*, 471.
[14] Y. Q. Zhu, W. K. Hsu, N. Grobert, B. H. Chang, M. Terrones, H. Terrones, H. W. Kroto, D. R. M. Walton, *Chem. Mater*. **2000**, *12*, 1190.
[15] M. Remskar, Z. Skraba, M. Regula, C. Ballif, R. Sanjinés, F. Lévy, *Adv. Mater*. **1998**, *10*, 246.
[16] M. Remskar, A. Mrzel, Z. Skraba, A. Jesih, M. Ceh, J. Demsar, P. Stadelmann, F. Lévy, D. Mihailovic, *Science* **2001**, *292*, 479.
[17] M. Nath C. N. R. Rao, *J. Am. Chem. Soc*. **2001**, *123*, 4841.
[18] J. Cumings A. Zettl, *Chem. Phys. Lett*. **2000**, *318*, 497.
[19] M. E. Spahr, P. Bitterli, R. Nesper, *Angew. Chem.* **1998**, *110*, 1339; *Angew. Chem. Int. Ed*. **1998**, *37*, 1263.
[20] G. B. Saupe, C. C. Waraksa, H-N Kim, Y. J. Han, D. M. Kaschak, D. M. Skinner, T. E. Mallouk, *Chem. Mater*. **2000**, *12*, 1556 – 1562.
[21] R. Abe, K. Shinohara, A. Tanaka, M. Hara, J. N. Kondo, K. Domen, *Chem. Mater*. **1997**, *9*, 2179.
[22] G. H. Du, Q. Chen, R. C. Che, Z. Y. Yuan, L.-M. Peng, *Appl. Phys. Lett*. **2001**, *79*, 3702.
[23] P. A. Parilla, A. C. Dillon, K. M. Jones, G. Riker, D. L. Schulz, D. S. Ginley, M. J. Heben, *Nature* **1999**, *397*, 114.
[24] F. Jensen H. Toftlund, *Chem. Phys. Lett*. **1993**, *201*, 89.
[25] D. Golberg, Y. Bando, O. Stéphan, K. Kurashima, *Appl. Phys. Lett*. **1998**, *73*, 2441.
[26] M. Terrones, W. K. Hsu, H. Terrones, J. P. Zhang, S. Ramos, J. P. Hare, R. Castillo, K. Prassides, A. K. Cheetham, H. W. Kroto, D. R. M. Walton, *Chem. Phys. Lett*. **1996**, *259*, 568.
[27] D. J. Srolovitz, S. A. Safran, M. Homyonfer, R. Tenne, *Phys. Rev. Lett*. **1995**, *74*, 1779.
[28] G. Seifert, H. Terrones, M. Terrones, G. Jungnickel, T. Frauenheim, *Phys. Rev. Lett*. **2000**, *85*, 146.
[29] A. Rubio, J. L. Corkill, M. L. Cohen, *Phys. Rev. B* **1994**, *49*, 5081.
[30] G. Seifert E. Hernandez, *Chem. Phys. Lett*. **2000**, *318*, 355.
[31] M. Cote, M, M. L. Cohen, D. J. Chadi, *Phys. Rev. B* **1998**, *58*, R4277.
[32] G. L. Frey, S. Elani, M. Homyonfer, Y. Feldman, R. Tenne, *Phys. Rev. B* **1998**, *57*, 6666.
[33] L. Scheffer, R. Rosentsveig, A. Margolin, R. Popovitz-Biro, G. Seifert, S. R. Cohen R. Tenne, *Phys. Chem. Chem. Phys.* **2002**, *4*, 2095.
[34] G. Seifert, H. Terrones, M. Terrones, T. Frauenheim, *Solid State Commun*. **2000**, *115*, 635.
[35] L. Rapoport, Yu. Bilik, Y. Feldman, M. Homyonfer, S. R. Cohen, R. Tenne, *Nature* **1997**, *387*, 791.
[36] M. Chhowalla G. A. J. Amaratunga, *Nature* **2000**, *407*, 164.
[37] L. Rapoport, M. Lvovsky, I. Lapsker, V. Leshchinsky, Yu Volovik, Y. Feldman, A. Margolin, R. Rosentsveig, R. Tenne, *Nano Lett.* **2001**, *1*, 137.
[38] J. Chen, N. Kuriyama, H. Yuan, H. T. Takeshita, T. Sakai, *J. Am. Chem. Soc*. **2001**, 123, 11813.
[39] J. Chen, S.-L. Li, Q. Xu, K. Tanaka, *Chem. Commun*. **2002**, 1722.

  0947-6539/02/0823-5304 $ 20.00+.50/0